Type of article: Original article

Title:

Zinc induces distinct changes in the metabolism of reactive oxygen and nitrogen species (ROS and RNS) in the roots of two *Brassica* species with different sensitivity to zinc stress

Gábor Feigl[1]*, Nóra Lehotai[1], Árpád Molnár[1], Attila Ördög[1], Marta Rodríguez-Ruiz[2], José M. Palma[2], Francisco J. Corpas[2], László Erdei[1], Zsuzsanna Kolbert[1]

[1]Department of Plant Biology, Faculty of Science and Informatics, University of Szeged, Szeged, Hungary

[2]Group of Antioxidants, Free Radicals and Nitric Oxide in Biotechnology, Food and Agriculture, Department of Biochemistry, Cell and Molecular Biology of Plants, Estación Experimental del Zaidín, CSIC, Granada, Spain

Running title: Zinc-induced changes in ROS and RNS metabolism of *Brassica* roots

Corresponding author: Gábor Feigl

Postal address: H-6726 Szeged, Közép fasor 52, Hungary

E-mail: fglgbr@gmail.com

Abstract

- *Background and Aims* Zinc (Zn) is an essential micronutrient present naturally in soils but it can be accumulated in the environment by anthropogenic activities provoking different types of damages to plants. Heavy metal stress stimulates the metabolism of reactive oxygen and nitrogen species (ROS and RNS) in different plant species. This study assesses the interplay of these two families of molecules to evaluate the putative nitro-oxidative stress response in roots of two *Brassica* species under high concentrations of zinc.
- *Methods* Nine-day-old hydroponically grown *Brassica juncea* and *Brassica napus* seedlings were treated with $ZnSO_4$ (0, 50, 150 and 300 μM) for seven days. Stress intensity was determined through the analyses of cell wall damages and cell viability. Key components of the metabolism of ROS and RNS including lipid peroxidation, enzymatic antioxidants, protein nitration and content of superoxide radical ($O_2^{\cdot -}$), nitric oxide (NO) and peroxynitrite ($ONOO^-$) were also measured through biochemical and cellular approaches.
- *Key Results* Under zinc stress, the analysis of morphological root damages and alterations of microelement homeostasis indicate that *B. juncea* is more tolerant to Zn stress than *B. napus*. On the other hand, ROS and RNS parameters suggest that the oxidative components are predominant compared to the nitrosative ones in the root system of both species.
- *Conclusions* The results indicate a clear relationship between ROS and RNS metabolisms as mechanism of response against an excess of zinc stress which provokes a nitro-oxidative stress. However, the oxidative stress components seem to be more dominant than the elements of the nitrosative stress in the root system of these two *Brassica* species.

Keywords

Brassica juncea, *Brassica napus*, excess zinc, reactive oxygen species, oxidative stress, reactive nitrogen species, nitrosative stress, protein nitration

Introduction

Heavy metal contamination is an increasingly serious problem for the environment and the agriculture. While according to the World Health Organisation, 31% of the world's population is potentially is at risk of zinc (Zn) deficiency (WHO 2005), the Zn contamination also appears to be a growing problem over the last decades (Zarcinas et al. 2004). The most important sources of zinc pollution in the environment are mostly anthropogenic, such as mining, waste disposal, electroplating or smelting (Bacon and Dinev 2005; Bi et al. 2006). Being an essential micronutrient, zinc plays an important role as a cofactor in numerous enzymes involved in protein synthesis and in carbohydrate, nucleic acid and lipid metabolism (Broadley et al. 2007). On the other hand, Zn excess may have a negative effect on plants. Among others, seed germination and plant growth inhibition (Mrozek and Funicelli 1982, Wang et al. 2009), changes in root development (Lingua et al. 2008), loss of membrane integrity (Stoyanova and Doncheva 2002) or cell death (Chang et al. 2005) were determined as the effects of zinc exposure. The mechanisms behind Zn toxicity are not completely understood; competition for catalytic sites or transporters (González-Guerrero et al. 2005), Zn-induced micronutrient-deficiency (Bonnet et al. 2000, Wang et al. 2009) or induction of oxidative stress (Wintz et al. 2003) were evidenced.

Non-redox active heavy metals such as zinc can cause oxidative stress by blocking essential functional groups in biomolecules because of their ability to bind strongly to oxygen, nitrogen or sulphur atoms, hereby inactivating enzymes by binding to their cysteine residues (Nieboer and Richardson 1980); or either able to replace another essential metal ions in their catalytic sites (Schützendübel and Polle 2002). During oxidative stress, reactive oxygen species (ROS), such as superoxide anion ($O_2^{\cdot -}$), hydrogen peroxide (H_2O_2), and hydroxyl radicals ($\cdot OH$) are

commonly generated. High levels of ROS are able to damage macromolecules, thus the ROS concentrations are needed to be strictly controlled by complex mechanisms in plants (Apel and Hirt, 2004). These include several enzymes such as ascorbate peroxidase (APX, EC 1.11.1.11), glutathione reductase (GR, EC 1.6.4.2), catalase (CAT, EC 1.11.1.6) superoxide dismutase (SOD, EC 1.1.5.1.1), and non-enzymatic, soluble antioxidants such as glutathione and ascorbate, among others.

Besides ROS, the term reactive nitrogen species (RNS) is extensively used to describe the family of nitric oxide (NO)-related molecules, such as peroxynitrite ($ONOO^-$), dinitrogen trioxide (N_2O_3), dinitrogen tetraoxide (N_2O_4), *S*-nitrosoglutathione (GSNO), nitrogen dioxide radical ($NO_2^{\cdot}$), nitrosonium cation (NO^+) and nitroxyl anion (NO^-) (Wang et al. 2013). Nitrosative stress as another stress process caused by environmental factors evolves as the consequence of RNS accumulation in the plant cells (Corpas et al 2007, 2011). However, the two families of reactive molecules (ROS and RNS) are involved in overlapping signalling processes; as a matter of fact the existence of nitro-oxidative stress has been reported to occur under certain circumstances (Corpas and Barroso 2013). An excellent example for the ROS-RNS crosstalk is the reaction between $O_2^{\cdot -}$ and NO yielding $ONOO^-$, which is responsible for the protein tyrosine nitration becoming a good biomarker of nitrosative stress in plants (Corpas et al 2007, 2013). Protein tyrosine nitration is a posttranslational modification resulting in an addition of a nitro group ($-NO_2$) to one of the two equivalent ortho carbons in the aromatic ring of tyrosine residues (Gow et al 2004). It causes steric and electronic perturbations, which modify the tyrosine's capability to function in electron transfer reactions or to keep the proper protein conformation (van der Vliet et al 1999). Tyrosine nitration can affect the function of a protein in numerous ways: besides no effect on functions or function gain, the most common result of tyrosine nitration is the inhibition of the protein's function (Greenacre and Ischiropoulos 2001; Radi 2004). Furthermore, tyrosine nitration has the ability

to influence several signal transduction pathways through the prevention of tyrosine phosphorylation (Galetskiy et al 2011).

In most plants, the vacuoles of the root cells serve as the most important Zn storage thus removing the metal from the root-shoot-leaf transport system and play a crucial role in basal Zn tolerance (Arrivault et al. 2006). Further protection mechanisms, like cell wall alterations, such as callose deposition are facilitating the survival of the plants by limiting the uptake and translocation of heavy metals and by preventing the leakage of assimilates and other nutrients (Sjölund 1997, Chen and Kim 2009). During callose deposition, the properties of the cell wall are modified by adding extra layers of carbohydrates synthesised by callose synthase, a transmembrane protein in the outer plasma membrane (Kartusch 2003).

Since heavy metals like zinc result in a massive loss of crop yield all over the world, the goal of this study was to investigate the morphological and physiological responses of two important crop plants, Indian mustard (*Brassica juncea*) and oilseed rape (*Brassica napus*) to zinc excess. Furthermore, our aim was to determine the potential involvement of ROS and RNS in the zinc sensitivity of *Brassica* species.

Materials and methods

Plant material and growing conditions

Brassica juncea L. Czern. and *Brassica napus* L. seeds were surface-sterilized with 5% (v/v) sodium hypochlorite and then placed onto perlite-filled Eppendorf tubes floating on full-strength Hoagland solution. The nutrient solution contained 5 mM $Ca(NO_3)_2$, 5 mM KNO_3, 2 mM $MgSO_4$, 1 mM KH_2PO_4, 0.01 mM Fe-EDTA, 10 μM H_3BO_3, 1 μM $MnSO_4$, 5 μM $ZnSO_4$, 0.5 μM $CuSO_4$, 0.1 μM $(NH_4)_6Mo_7O_{24}$ and 10 μM $AlCl_3$. Seedlings were precultivated for nine days – until the appearance of the first leaves – and then the nutrient solution was changed and supplemented with 0 (control), 50, 150 and 300 μM $ZnSO_4$ for seven days. Control plants were grown in full strength Hoagland solution containing 5 μM $ZnSO_4$. The plants were kept in a greenhouse at a photon flux density of 150 μmol m^{-2} s^{-1} (12/12h light/dark cycle) at a relative humidity of 55-60% and 25±2°C for seven days.

All chemicals used during the experiments were purchased from Sigma-Aldrich (St. Louis, MO, USA) unless stated otherwise.

Element content analysis

The concentrations of microelements were measured by using inductively coupled plasma mass spectrometry (ICP-MS, Thermo Scientific XSeries II, Asheville, USA) according to Lehotai et al. (2012). Root and shoot material of control, 50, 150 and 300 μM Zn-treated *B. juncea* and *B. napus* were harvested separately and rinsed with distilled water to remove the potentially attached Zn from their surface. After 72 h of drying at 70°C, 65% (w/v) nitric acid

and 30% (w/v) hydrogen peroxide (both from Reanal, Budapest, Hungary) were added to the samples, which were subjected to 200°C and 1600W for 15 min. Values of Zn and other microelement concentrations are given in μg g^{-1} dry weight (DW).

Morphological measurements

Fresh weights (g) of the root material were measured on the 7th day of the treatment using a balance. The length of the primary root (cm) and the first six lateral roots from the root collar (cm) were also determined manually. Also the visible lateral roots were counted and their number is expressed as pieces/root. The root fresh weight and the primary root length are expressed as % of control.

Microscopic determination of zinc distribution, callose deposition, lipid peroxidation and viability loss in the root tissues

For visualisation of Zn, root tips were equilibrated in PBS buffer (137 mM NaCl, 2.68 mM KCl, 8.1 mM Na_2HPO_4, 1.47 mM KH_2PO_4, pH 7.4), and further incubated with 25 μM Zinquin (ethyl (2-methyl-8-p-toluenesulphonamido-6-quinolyloxy)acetate) in PBS for 1 h at room temperature in darkness according to Sarret et al. (2006). Callose deposition in the root tissues was determined by image analysis using aniline blue according to Cao et al. (2011) with slight modifications. Root samples were incubated in aniline blue solution (0.1%, w/v in 1M glycine) for 5 min, and then washed once with distilled water. Products of lipid peroxidation (such as malondialdehydes) were visualized using Schiff's reagent, according to Arasimowicz-Jelonek et al. (2009). Root tips were incubated in the dye solution for 20 minutes and then the reagent was replaced by 0.5% (w/v) $K_2S_2O_5$ (prepared in 0.05M HCl) for

a further 20 minutes. For the determination of cell viability in the root tips, fluorescein diacetate (FDA) staining was used according to Lehotai et al. (2011). Root segments were incubated in 10 μM dye solution prepared in 10 mM MES (4-morpholineethanesulfonic acid) buffer (pH 6.15) containing 50 mM KCl, then they were washed four times with MES/KCl.

Detection of reactive oxygen- (ROS) and nitrogen species (RNS)

Dihydroethidium (DHE) was used for visualisation of superoxide anion contents in the root tips, which were incubated for 30 min in darkness at 37°C in 10 μM dye solution and were washed twice with 10 mM Tris/HCl , pH 7.4 (Kolbert et al., 2012). For hydrogen peroxide detection, root segments were incubated in 50 μM Ampliflu™ (10-acetyl-3,7-dihydroxyphenoxazine, ADHP or Amplex Red) solution and washed with 50 mM sodium phosphate buffer, pH 7.5, according to Lehotai et al. (2012). The NO levels in *Brassica* root tips were determined by 4-amino-5-methylamino-2',7'-difluorofluorescein diacetate (DAF-FM DA) (Kolbert et al., 2012). Root segments were incubated for 30 min in darkness at room temperature in 10 μM dye solution, and were washed twice with 10 mM Tris/HCl buffer, pH 7.4. Although DAF-FM DA allows only semi-quantitative analysis, it is a reliable fluorophore for *in situ* detection of NO in plant tissues, since it does not react with hydrogen peroxide or peroxynitrite, but it responds to NO donors and/or scavengers (Kolbert et al., 2012). For the *in situ* and *in vivo* detection of peroxynitrite ($ONOO^-$), 3'-(*p*-aminophenyl) fluorescein (APF) was applied (Chaki et al., 2009). The $ONOO^-$- sensitivity of APF was proved *in vitro*, and it was also shown that the dye does not react with NO or H_2O_2 (Kolbert et al., 2012). Root samples were incubated in darkness at room temperature in 10 μM dye solution for 1 h and were washed twice with 10 mM Tris/HCl buffer, pH 7.4.

The roots of *Brassica* plants labelled with different fluorophores were investigated under a Zeiss Axiovert 200M inverted microscope (Carl Zeiss, Jena, Germany) equipped with filter set 9 (exc.: 450-490 nm, em.: 515- ∞ nm) for DHE, filter set 10 (exc.: 450-490, em.: 515-565 nm) for APF, DAF-FM and FDA, filter set 20HE (exc.: 546/12, em.: 607/80) for Amplex Red, or filter set 49 (exc.: 365 nm, em.: 445/50 nm) for aniline blue and Zinquin. Fluorescence intensities (pixel intensity) in the meristematic zone of the primary roots were measured on digital images using Axiovision Rel. 4.8 software within circles of 100 µm radii.

Visualization of intracellular zinc compartmentalization by confocal laser scanning microscopy (CLSM)

Root samples were washed three times alternately in deionized water and in 10 mM ethylenediaminetetraacetic acid (EDTA) before being incubated in 20 µM Zinpyr-1 solution (in PBS) at room temperature in darkness for 3 h (Sinclair et al. 2007). Samples were rinsed in deionized water, and immersed in 10 µM propidium iodide to label cell walls (Tsukagoshi et al. 2010). Samples were mounted in PBS and images were taken on a CLS microscope (Olympus LSM 700, Olympus, Tokyo, Japan) using excitation at 488 nm with a 100mW Ar ion laser and a ×20 Plan Apo water immersion lens with fluorescein isothiocyanate (FITC) and PI filters. Images were processed with Olympus Fluoview FV100 software and were analysed using Fiji software (http://fiji.sc/Fiji, Schindelin et al., 2012).

Measurement of the enzymatic antioxidant activity

SOD (EC 1.15.1.1) activity was determined by measuring the ability of the enzyme to inhibit the photochemical reduction of nitro blue tetrazolium (NBT) in the presence of riboflavin in light (Dhindsa et al., 1981). For the enzyme extract, 250 mg plant material was grinded with

10 mg polyvinyl polypyrrolidone (PVPP) and 1 ml 50 mM phosphate buffer (pH 7.0, with 1 mM EDTA added). The enzyme activity is expressed in Unit · g^{-1} fresh weight; one unit (U) of SOD corresponds to the amount of enzyme causing a 50% inhibition of NBT reduction in light.

Activity of ascorbate peroxidase (APX; EC 1.11.1.11) was measured by monitoring the decrease of ascorbate content at 265 nm (ε=14 mM^{-1} cm^{-1}) according to a modified method by Nakano and Asada (1981). For the enzyme extract, 250 mg plant material was grinded with 1.5 ml extraction buffer containing 1mM EDTA, 50mM NaCl and 900 µM ascorbate. Data are expressed as activity (Unit · g^{-1} fresh weight).

SOD activity on native PAGE, isoform staining

SOD isoforms were detected in gels by the modified method of Beauchamp and Fridovich (1971). SOD isozymes were separated by non-denaturating PAGE on 10% acrylamide gels, followed by incubating sequentially in 2.45 mM NBT for 20 min and in 28 µM riboflavin and 28 mM tetramethyl ethylene diamine (TEMED) for 15 min in darkness. Colourless SOD bands on a dark blue background were observed after light exposure. SOD isoforms were identified by incubating gels in 50 mM potassium phosphate buffer (pH 7.0) supplemented with 3 mM KCN (inhibits Cu/Zn SOD) or 5 mM H_2O_2 (inhibits both Cu/Zn- and Fe-SOD) for 30 min before staining with NBT. Mn-SODs are resistant to both inhibitors.

Immunoprecipitation, SDS-PAGE and Western blotting

Crude extracts from plant material were immunoprecipitated by using Thermo Scientific Pierce Crosslink Magnetic IP/Co-IP Kit (Hudson, NH, USA). The beads were cross-linked

with antibody against 3-nitrotyrosine. After purification, immunoprecipited samples were subjected to sodium dodecyl sulphate-polyacrylamide gel electrophoresis (SDS-PAGE) on 12% acrylamide gels. For western blot analysis, proteins were transferred to PVDF membranes using the wet blotting procedure. After transfer, membranes were used for cross-reactivity assays with rabbit polyclonal antibody against 3-nitrotyrosine diluted 1:2000 (Corpas et al. 2008). Immunodetection was performed by using affinity isolated goat anti-rabbit IgG-alkaline phosphatase secondary antibody in dilution of 1:10 000, and bands were visualised by using NBT/BCIP reaction. As a positive control nitrated bovine serum albumin was used.

Statistical analysis

All experiments were carried out at least two times. In each treatment at least 10-20 samples were measured. The results are expressed as mean ± SE. Multiple comparison analyses were performed with SigmaStat 12 software using analysis of variance (ANOVA, $P<0.05$) and Duncan's test. In some cases, Microsoft Excel 2010 and Student's t-test were used (*$P\leq0.05$, **$P\leq0.01$, ***$P\leq0.001$).

Results and discussion

Zinc uptake, accumulation and microelement homeostasis in *Brassica* species

Increasing zinc concentrations in the nutrient solutions promoted significant increases of zinc content of the root system in both species (Fig 1A). The two *Brassica* species showed no differences in their zinc uptake capacity; although in case of the highest zinc treatment *B. juncea* accumulated slightly (~14%) more metal in its root system. Regarding to the shoots, the treatments resulted in a concentration-dependent response of zinc content; however the values were lower by one order of magnitude than in the root. Moreover, the shoot system of *B. napus* contained higher (~48, ~33 and ~14%, respectively) zinc levels compared to that of *B. juncea* (Fig 1B). Results suggest an efficient root-to-shoot zinc translocation in both species; however *B. napus* showed a better transport capacity to the aerial parts in case of all zinc treatments. Zinc is predominantly complexed with citric and malic acid in the xylem sap. Moreover, small amounts of soluble Zn-phosphate were also found in the sap in case of excess Zn (White et al. 1981). In our experimental system, the *Brassica* species at their early developmental stage (16 days-old plants) proved to be zinc accumulators, since the transported amount of Zn is more than 0.1% of the shoot dry weight. Similar Zn accumulation tendencies were found in the roots and shoots of 12-days-old *Brassica* ssp., which were considered to be as moderate zinc accumulators with some potentiality for phytoremediation (Ebbs and Kochian 1997).

Besides zinc, the concentrations of other microelements (Cu, Mn, Fe) were also determined in the roots of *Brassica* species using the ICP-MS technique (Table 1). The applied Zn treatments resulted in elevated copper contents in the root system of both *Brassica* species

compared to the control. The lack of the zinc-copper antagonism can be explained by the discrimination between the divalent ions (Irving-Williams order). Zinc and copper use the same transporters, which can be up-regulated by Zn excess, although they prefer Cu more than Zn (Fraústo da Silva and Williams 2001). This can trigger the increase in Cu content in the two zinc-exposed B*rassica* species. Similarly to copper, iron contents of the root system showed a slight but significant increase in both species as the effect of zinc. In contrast, all the applied zinc concentrations led to the strong decrease of manganese content in the roots of both species. In *Arabidopsis thaliana* and *Thlaspi caerulescens* roots, zinc caused similar changes of iron and manganese contents (van de Mortel et al. 2006). Moreover, also in the roots of zinc-exposed *Lolium perenne* the manganese contents were significantly reduced (Monnet et al. 2001). The synergistic effect we found between iron and zinc suggests that both species may increase their iron uptake in order to avoid iron deficiency in leaves. In *Arabidopsis* roots, Zn excess notably induced the expression of the ferric-chelate reductase gene (FRO2), which contributed to the intensification of Fe uptake (van de Mortel et al. 2006). In the case of manganese, an antagonistic relationship with zinc seems to be the rule in the roots of both species.

Tissue-specific and subcellular localization of zinc in the root of *Brassica* species

The tissue localization pattern of zinc in the root tips was visualized by Zinquin fluorophore. Homogenous, low-level Zn-dependent fluorescence was detected in the root tips of control plants. As the effect of the increasing external Zn concentration, the accumulation of the fluorescent signal was the most evident in the meristematic and transition zones (Fig 2), probably because of the greater permeability of the thin walls of meristem cells for zinc ions. In the cells of the elongation zone, lower fluorescence intensity was observed, while in the

differentiation zone the zinc-associated fluorescence intensified as the effect of external treatments and also the root hairs showed zinc content (see Fig 2A). Similarly, in the root tips of *Solanum nigrum*, zinc exposition (400 μM $ZnCl_2$) caused the intensification of Zinquin fluorescence, but this fluorescent signal showed homogenous distribution within the tip (Xu et al. 2010). Although practically there were no difference between the zinc contents of the whole root system of the species (see Fig 1A), the Zinquin fluorescence of the meristematic zones proved to be higher in zinc-treated *B. juncea* (Fig 2B), which suggests the higher accumulation of zinc in those root tips compared to *B. napus*. The increment of the fluorescent signal proved to be concentration-dependent neither in *B. juncea* nor in *B. napus* (Fig 2B).

Subcellular zinc distribution within the root cells of zinc-treated *Brassica* was investigated by confocal microscopy in order to reveal the role of the cell wall in zinc binding. The zinc-dependent green fluorescence was the most intense in the walls of the epidermal cell layer of the root. Zinc localized also in the cytoplasm and/or in vacuoles and around the surface of the nuclei of these cells, which showed also PI-dependent fluorescence, suggesting that these cells are not viable. The localization of zinc in the root cell nuclei of zinc-exposed plants was shown also by Rathore et al. (1972). In the inner cell layers of the root, mainly the apoplast possessed zinc content, and most of the cells were alive (Fig 3). Similarly to the results of Küpper et al. (2000), root epidermal cells accumulate zinc mostly in their walls. The cell wall metabolic inactivity provides advantage for metal precipitation and exclusion from the cytoplasm (Krzesłowska 2011), which can ensure the survival in case of metal excess (Rout and Das 2003). Some early works suggested that zinc is associated with the carbohydrate components of the cell wall such as hemicelluloses and pectins (Diez-Altares and Bornemisza 1967, Turner and Marshall 1972). Recent studies revealed that low-methylesterified pectins are the most important metal-binding components of the cell wall (Krzesłowska 2011). The

epidermal cells suffer from cell death presumably because of the presence of zinc also in their cytoplasm, while the inner cells (cortex) contain less zinc mainly in their walls and they remain viable.

Zinc-triggered changes in root architecture

With the increasing Zn concentrations, leaf area, fresh and dry weight of the shoot significantly decreased (data not shown) and chlorosis was also visible (Fig 4A). However, necrotic lesions on the leaf blades were not observed during the experimental period. Root system has a great importance during the life of the heavy metal-exposed plants, since it can contribute to tolerance e.g. by controlling metal uptake or storage of excess metal. These support the necessity of the detailed investigation of the root development, which revealed differences between the *Brassica* species. The root tip morphology was modified by zinc excess, since the meristematic and transition zones were narrower, while the diameter of the upper regions was visibly larger than in the control root (see Fig 2A). This zinc-induced morphological alteration was observed in both species, but it was more evident in case of *B. napus*. Moreover, root hair formation was remarkably induced by zinc excess especially in *B. napus* roots (see Fig 2A). Interestingly, the primary root (PR) elongation of *B. juncea* was not notably affected by zinc, while in case of *B. napus* it was significantly inhibited at all applied zinc concentrations (Fig 4B). Mild stress (50 μM $ZnSO_4$) resulted in a notable elevation of lateral root (LR) number in both species. Similarly, 150 μM $ZnSO_4$ increased the number of LRs, but the effect was much slighter in this case. Moreover, the highest applied Zn concentration did not affect the LR development of the species (Fig 4C). The length of the lateral roots was remarkably diminished by zinc exposure in both *Brassica* species; however the rate of the inhibition proved to be lower in 50 μM zinc-treated *B. juncea* than in *B. napus*

(Fig 4D). Based on these data, the cell elongation and division processes in the primary and lateral roots are more sensitive to zinc excess than the anticlinal divisions of the pericycle cells during LR initiation. Indeed, the PR tips of zinc-treated sugarcane showed significantly reduced mitotic index and wide spectrum of cytotoxic effects (Jain et al. 2010). The fresh weight of the root system showed zinc-induced reduction only in *B. napus*, while in *B. juncea* zinc stress was not able to alter the fresh root biomass (Fig 4E). Results show that zinc excess modifies the root system architecture depending on its concentration and the effect was different in the species. Namely, mild zinc exposure (50 μM $ZnSO_4$) triggered the development of stress-induced morphogenetic response (SIMR) phenotype (Potters et al. 2009) only in *B. napus*, since it resulted in shorter PR and larger amount of (shorter) LRs. Similar stress-induced root development was observed e.g. in selenium or copper exposed *Arabidopsis* or chromium treated wheat plants (Lehotai et al. 2012, Pető et al. 2011, Hasnain et al. 1997). In contrast, in *B. juncea* LR formation was induced (more significantly than in *B. napus*) and the PR elongation was not affected by zinc stress, which led to the development of an extended root system compared to the control plants. It can be assumed that these developmental changes can be parts of the acclimation process, because they can ensure better nutrient and water uptake thus survival of the *B. juncea* plant.

Zinc stress provokes changes in the cell wall structure

Cell wall alterations, such as lignification or callose deposition, can help the plant cells tolerating excess heavy metal (HM) by serving as a physical barrier, thus preventing the heavy metals entering the cytoplasm. Besides their role in HM tolerance these cell wall modifications can partly be responsible for growth diminution as well.

Under copper stress a hydrogen peroxide-dependent lignin formation in the lateral roots of both *Brassica* species was found (Feigl et al. 2013), but zinc-induced lignification was not detectable in the root system (data not shown). On the other hand, the results show that excess Zn caused significant callose deposition in the roots of both species and this callose content increment was more pronounced in *B. napus* (Fig 5). Similarly, callose accumulation was observed in zinc-treated bean plants (Peterson and Rauser 1979). The deposited callose could inhibit root growth by decreasing cell wall loosening, thus preventing the passage of signal molecules or inhibit the symplastic supply of carbon required for root growth (Jones et al. 2006, Piršelová et al. 2012). In comparison, there was not significant callose deposition induced by copper stress either in *B. juncea* or in *B. napus* (Feigl et al. 2013), so hereby we can state that this cell wall modification is a heavy metal-dependent process, but it is independent from the plant species.

The *Brassica* species show different sensitivity to zinc stress

We characterized the degree of zinc sensitivity by detecting the viability of the root meristem (fluorescein diacetate labelling) and calculating the tolerance index (%) based on PR elongation. The root meristem cells of *B. juncea* remained fully viable even in case of 300 μM $ZnSO_4$ treatment, while root meristem of *B. napus* underwent significant viability loss as the effect of zinc exposure (Fig 6). Based on the results, the viability status of the primary root meristem cells are in accordance with the elongation capability of the root (see Fig 4B). The tolerance indexes of zinc-treated *B. juncea* showed no decrease at higher concentrations of external Zn (Control: 100%, 50 μM $ZnSO_4$: 97%, 150 μM $ZnSO_4$: 119% and 300 μM $ZnSO_4$: 107%); however they significantly decreased in case of zinc-exposed *B. napus* (Control: 100%, 50 μM $ZnSO_4$: 61%, 150 μM $ZnSO_4$: 50% and 300 μM $ZnSO_4$: 52%). The results

show that *B. juncea* possesses remarkable zinc tolerance compared to *B. napus*, which supports the species specificity of zinc sensitivity.

Altered metabolism of ROS and RNS in Zn-exposed *Brassica* species

The effect of zinc excess on the ROS, RNS and antioxidants levels was accomplished in this work. In the roots of *B. juncea*, the level of superoxide anion significantly decreased as a consequence of zinc excess (Fig 7A), which can be explained by the enhancement of SOD activity (Fig 7B). In contrast, superoxide levels of 50 and 150 μM Zn-treated *B. napus* roots showed a significant increment, which was accompanied by the increased SOD activity. These suggest that the elevated SOD activity was not able to compensate the formation of superoxide anion in case of 50 and 150 μM Zn; although it could reduce the superoxide content during severe Zn stress (300 μM). We separated the different SOD isoforms by native PAGE and five activity bands were identified in case of both species (Fig 8). The obtained pattern is in agreement with the result published by Cohu and Pilon (2007) in case of *B. juncea*, however we found a different configuration of SOD isoforms in *B. napus* than it was published by Abedi and Paniyat (2010). The experiments with specific inhibitors showed that the uppermost band represented a Mn-SOD isoform, which activity decreased by the increasing Zn concentrations in both species, but especially in *B. napus*. The diminution of Mn-SOD activity can be explained by the reduced availability of manganese as previously showed in Table 1. The Fe-SOD isoform was only hardly visible in case of *B. juncea* and only present in the control sample of *B. napus*. The last three bands showed Cu/Zn-SODs, which strengths were in correlation with the overall SOD activity (see Fig 6B). Similarly to our results, the decrease of the activity of all three isoenzymes was published e.g. in cadmium-exposed pea plants (Sandalio et al. 2001).

The level of H_2O_2 remained low in zinc-treated *B. juncea* (Fig 7C), and the pattern of APX activity (Fig 7D) could partly explain the hydrogen peroxide profile. On the contrary, in *B. napus* the highest applied Zn concentration resulted in an extreme H_2O_2 accumulation, but APX did not vary comparing to control plants (Fig 7C and D, respectively). As it has been reported earlier, zinc-triggered ROS formation and modification of antioxidant capacity was published e.g. in sugarcane, bean, maize or pea (Jain et al. 2010, Chaoui et al. 1997, Lozano-Rodríguez et al. 1997).

In the root tips of both examined species, NO formation was detectable in a concentration-dependent manner; however this elevation was statistically significant only in the roots of *B. juncea* (Fig 7E). Several possible mechanisms of NO formation can exist in this system. Xu et al. (2010) published that zinc-induced Fe-deficiency can be partially responsible for NO production in *Solanum nigrum* root tips, although in our experiments, zinc-induced Fe deficiency was not observed (see Table 1). The major enzymatic source of NO in the roots is nitrate reductase, but this activity was not influenced by zinc excess in *Brassica* roots (Bartha et al. 2005). Furthermore, the transition metal-triggered decomposition of NO pools such as S-nitrosoglutathione (Smith and Dasgupta 2000) may result in NO liberation in Zn-exposed *Brassica* roots, but this possibility remains to be elucidated. Nitric oxide may react with superoxide anion yielding peroxynitrite ($ONOO^-$), a powerful oxidative and nitrosative agent (Arasimowicz-Jelonek and Floryszak-Wieczorek 2011). The significant zinc-induced enhancement of peroxynitrite content in both species (Fig 7F) may explain the moderate NO accumulation, since part of the formed NO possibly transformed into peroxynitrite. This hypothesis can be supported by the decreasing superoxide levels in *B. juncea* (Fig 7B); while in *B. napus* superoxide levels remained high (Fig 7B) and less peroxynitrite is perhaps being produced through this pathway (Fig 7F). The SOD system is possibly playing an important role in the regulation of the peroxynitrite formation, by modulating the levels of superoxide

radicals driven to this reaction. The representative fluorescent microscopic images of the root tips stained with different fluorophores can be seen in Fig 7G.

The significant and zinc concentration-dependent peroxynitrite formation in both species predicted protein tyrosine nitration and, therefore, this event was studied by Western blot analysis using an antibody against nitro-tyrosine (Fig 9). The presence of seven nitrotyrosine-immunopositive protein bands in the untreated samples suggests that a part of the protein pool is nitrated even under control circumstances. Similarly, a basal nitration state of proteins was published in different plant species such as sunflower, *Citrus* and pea (see Chaki et al., 2009; Begara-Morales et al 2013; Corpas et al. 2013). We observed strengthening of the same seven protein bands due to the effect of 300 μM $ZnSO_4$, which suggests the intensification of protein nitration induced by zinc excess. The enhancement of nitration levels was pronounced in both species, which implies that the proteome of both species are sensitive to nitrosative modification. Similarly, intensified tyrosine nitration was observed in salt-stressed olive leaves as well as in leaves of cold-treated pea or in water-stressed *Lotus japonicus* (Corpas et al. 2008, Valderrama et al. 2006 Signorelli et al. 2013); however to our knowledge this is the first which demonstrates heavy metal-induced protein nitration.

Peroxynitrite - through the formation of peroxynitrous acid (ONOOH) - can lead to lipid peroxidation, which product – malondialdehyde (MDA) - can be detected *in situ* by histochemically (Arasimowicz-Jelonek et al. 2009). During the microscopic investigation using the Schiff's staining procedure, the root tips of *B. napus* showed slight but visible pink colorization reflecting the zinc-induced increment of the MDA content (Fig 10). In contrast, zinc-treated B. juncea root tips remained unstained. These suggest that the root tip cells of *B. napus* suffered oxidative membrane damage, while in the root tips of *B. juncea* there was no detectable lipid peroxidation.

Conclusions

Taken together, these results clearly show that the morphological and physiological responses of *Brassica* species to zinc stress are different. In the roots *B. juncea*, possessing better zinc resistance, only a slight ROS formation, activation of antioxidant enzymes (SOD, APX) and no remarkable lipid peroxidation were observed, which reflect the lack of a zinc-induced serious oxidative stress. Although, the significant production of RNS (NO and $ONOO^-$) and the occurrence of protein nitration reveal a zinc-triggered secondary, nitrosative stress in *B. juncea*. Contrary, as the effect of zinc exposure, nitro-oxidative stress occurred in the more sensitive *B. napus* as a consequence of ROS and RNS accumulation, lipid peroxidation and protein tyrosine nitration. Our data reveal the existence of a relationship between ROS and RNS metabolism under zinc stress and the contribution of nitro-oxidative stress to zinc sensitivity. The results also suggest that sensitivity to zinc is determined rather by the level of oxidative than by the nitrosative processes in *Brassica* species.

Funding

This research was supported by the European Union and the State of Hungary, co-financed by the European Social Fund in the framework of TÁMOP 4.2.4. A/2-11-1-2012-0001 'National Excellence Program'. The infrastructural background and the purchasing of consumables were ensured by the Hungarian Scientific Research Fund (Grant no. OTKA PD100504).

Projects AGL2011-26044 and BIO2012-33904 from the Ministry of Economy and Competitiveness (Spain) are also acknowledged.

Acknowledgements

The technical assistance of Carmelo Ruiz, Estación Experimental del Zaidín, Granada, Spain is also acknowledged.

Literature cited

Abedi T, Pakniyat H. 2010. Antioxidant enzyme changes in response to drought stress in ten cultivars of oilseed rape (*Brassica napus* L.). *Czech J. Genet. Plant Breed*, **46**(1), 27-34.

Apel K, Hirt H. 2004. Reactive oxygen species: metabolism, oxidative stress, and signal transduction. *Annu. Rev. Plant Biol*., **55**, 373-399.

Arasimowicz-Jelonek M, Floryszak-Wieczorek J. 2011. Understanding the fate of peroxynitrite in plant cells--from physiology to pathophysiology. *Phytochemistry*, **72**(8), 681-688

Arrivault S, Senger T, Krämer U. 2006. The *Arabidopsis* metal tolerance protein AtMTP3 maintains metal homeostasis by mediating Zn exclusion from the shoot under Fe deficienc and Zn oversupply. *Plant J*. **46** (5) 861-879.

Bacon JR, Dinev NS. 2005. Isotopic characterization of lead in contaminated soils from the vicinity of a non-ferrous metal smelter near Plodviv, Bulgaria. *Environ. Pollut*. **134**, 247-255.

Bartha B, Kolbert Zs, Erdei L. 2005. Nitric oxide production induced by heavy metals in *Brassica juncea* L. Czern. and *Pisum sativum* L. *Acta Biol Szeged*, **49**(1-2), 9-12.

Beauchamp C, Fridovich I. 1971. Superoxide dismutase: improved assays and an assay applicable to acrylamide gels. *Analytical biochemistry*, **44**(1), 276-287.

Bi X, Feng X, Yang Y, Qiu G, Li G, Li F, Liu T, Fu Z, Jin Z. 2006. Environmental contamination of heavy metals from zinc smelting areas in Hezhang County, western Guizhou, China. *Environ. Int*. **32**, 883-890.

Bonnet M, Camares O, Veisseire P. 2000. Effects of zinc and influence of *Acremonium lolii* on growth parameters, chlorophyll a fluorescence and antioxidant enzyme activities of ryegrass (*Lolium perenne* L. cv. Apollo). *J Exp Bot* **346**: 945–953

Broadley MR, White PJ, Hammond JP, Zelko I, Lux A. 2007. Zinc in plants. *New Phytol* **173**: 677–702

Cao P, Sun J, Zhao P, Liu H, Zheng G. 2011. A new putative plasmodesmata protein, At1g19190 in *Arabidopsis*. *Afr. J. Biotech*. **10**, 17409-17423

Chaki M, Valderrama R, Fernández-Ocaña AM, Carreras A, López-Jaramillo J, Luque F, Palma JM, Pedrajas JR, Begara-Morales JC, Sánchez-Calvo B, Gómez-Rodríguez MV, Corpas FJ, Barroso JB. 2009. Protein targets of tyrosine nitration in sunflower (*Helianthus annuus* L.) hypocotyls. *J Exp Bot*. **60**:4221-34.

Chang HB, Lin CW, Huang HJ. 2005. Zinc-induced cell death in rice (*Oryza sativa* L.) roots. *Plant Growth Regul*. **46**, 261–266.

Chaoui A, Mazhoudi S, Ghorbal MH, Elferjani E. 1997. Cadmium and zinc induction of lipid peroxidation and effects on antioxidant enzyme activities in bean (*Phaseolus vulgaris* L.). *Plant Sci* **127**:139–147

Chen XY, Kim JY. 2009. Callose synthesis in higher plants. *Plant Signal Behav*, **4**(6), 489-492.

Cohu CM, Pilon M. 2007. Regulation of superoxide dismutase expression by copper availability. *Physiologia Plantarum*, **129**(4), 747-755.

Corpas FJ, Barroso JB. 2013. Nitro-oxidative stress vs oxidative or nitrosative stress in higher plants. New Phytologist, 199(3), 633-635.

Corpas FJ, Chaki M, Fernández- Ocaña A, Valderrama R, Palma JM, Carreras A, Begara-Morales JC, Airaki M, del Río LA, Barroso JB. 2008. Metabolism of Reactive Nitrogen Species in Pea Plants Under Abiotic Stress Conditions. *Plant Cell Physiol* (2008b) **49** (11):1711-1722

Corpas FJ, del Río LA, Barroso JB. 2007. Need of biomarkers of nitrosative stress in plants. *Trends in Plant Science* **12**: 436-438.

Corpas FJ, Palma JM, del Río LA, Barroso JB. 2013. Protein tyrosine nitration in higher plants grown under natural and stress conditions. *Front. Plant Sci*. **4** (2013)

Diez-Altares C, Bornemisza E. 1967. The localization of zinc-65 in germinating corn tissues. *Plant and Soil*, **26**(1), 175-188.

Dhindsa RS, Plumb-Dhindsa P, Thorpe TA. 1981. Leaf senescence: correlated with increased levels of membrane permeability and lipid peroxidation, and decreased levels of superoxide dismutase and catalase. *J. Exp. Bot*. **32**, 93–101.

Ebbs SD, Kochian LV. 1997. Toxicity of zinc and copper to *Brassica* species: implications for phytoremediation. *Journal of Environmental Quality*, **26**(3), 776-781.

Feigl G, Kumar D, Lehotai N, Tugyi N, Molnár Á, Ördög A, Szepesi Á, Gémes K, Laskay G, Erdei L, Kolbert Zs. 2013. Physiological and morphological responses of the root system of Indian mustard (*Brassica juncea* L. Czern.) and rapeseed (*Brassica napus* L.) to copper stress. *Ecotoxicology and environmental safety*, **94**, 179-189.

Fraústo da Silva JJR, Williams RJP. 2001. The Biological Chemistry of the Elements, 2nd edn. Clarenton Press, Oxford, UK

Galetskiy D, Lohscheider JN, Kononikhin AS, Popov IA, Nikolaev EN, Adamska I. 2011. Phosphorylation and nitration levels of photosynthetic proteins are conversely regulated by light stress. Plant Mol. Biol. 77, 461-473.

González-Guerrero M, Azcón-Aguilar C, Mooney M, Valderas A, MacDiarmid CW, Eide DJ, Ferrol N. 2005. Characterization of a *Glomus intraradices* gene encoding a putative Zn transporter of the cation diffusion facilitator family. *Fungal Genet Biol* **42**: 130–140

Gow AJ, Farkouh CR, Munson DA, Posencheg MA, Ischiropoulos H. 2004. Biological significance of nitric oxide-mediated protein modifications. *Am. J. Physiol. Lung Cell Mol. Physiol.* **287**, L262-L268.

Greenacre SA, Ischiropoulos H. 2001. Tyrosine nitration: localisation, quantification, consequences for protein function and signal transduction. *Free Radic. Res*. **34**, 541-581

Hasnain S, Sabri AN. 1997. Growth stimulation of *Triticum aestivum* seedlings under Cr-stresses by non-rhizospheric pseudomonad strains. *Environmental pollution*, **97**(3), 265-273.

Jain R, Srivastava S, Solomon S, Shrivastava AK, Chandra A. 2010. Impact of excess zinc on growth parameters, cell division, nutrient accumulation, photosynthetic pigments and oxidative stress of sugarcane (*Saccharum* spp.). *Acta physiologiae plantarum*, **32**(5), 979-986.

Jones DL, Blancaflor EB, Kochian LV, Gilroy S. 2006. Spatial coordination of aluminium uptake, production of reactive oxygen species, callose production and wall rigidification in maize roots. *Plant, cell & environment*, **29**(7), 1309-1318.

Kartusch R. 2003. On the mechanism of callose synthesis induction by metal ions in onion epidermal cells. *Protoplasma* **220**, 219-225.

Kolbert Zs, Pető A, Lehotai N, Feigl G, Ördög A, Erdei L. 2012. In vivo and in vitro studies on fluorophore-specificity. *Acta Biol. Szeged*. **56**, 37-41.

Küpper H, Lombi E, Zhao FJ, McGrath SP. 2000. Cellular compartmentation of cadmium and zinc in relation to other elements in the hyperaccumulator *Arabidopsis halleri*. *Planta* **212**(1), 75-84.

Krzesłowska M. 2011. The cell wall in plant cell response to trace metals: polysaccharide remodeling and its role in defense strategy. *Acta physiologiae plantarum*, **33**(1), 35-51.

Lehotai N, Kolbert Zs, Pető A, Feigl G, Ördög A, Kumar D, Tari I, Erdei L. 2012. Selenite-induced hormonal and signalling mechanisms during root growth of *Arabidopsis thaliana* L. *J. Exp. Bot*. **63**, 5677-5687.

Lingua G, Franchin C, Todeschini V, Castiglione S, Biondi S, Burlando B, Parravicini V, Torrigiani P, Berta G. 2008. Arbuscular mycorrhizal fungi differentially affect the response to high zinc concentrations of two registered poplar clones. *Environ. Pollut*. **153**, 137–147.

Lozano-Rodriguez E, Hernandez LE, Bonay P, Carpena-Ruiz RO. 1997. Distribution of cadmium in shoot and root tissues of maize and pea plants: physiological disturbances. *J Exp Bot* **48**:123–128

Monnet F, Vaillant N, Vernay P, Coudret A, Sallanon H, Hitmi A. 2001. Relationship between PSII activity, CO_2 fixation, and Zn, Mn and Mg contents of *Lolium perenne* under zinc stress. *Journal of Plant Physiology*, **158**(9), 1137-1144.

Mrozek JE, Funicelli NA. 1982. Effect of zinc and lead on germination of *Spartina alterniflora* Loisel seeds at various salinities. *Environ. Exp. Bot*. **22**, 23-32.

Nakano Y, Asada K. 1981. Hydrogen peroxide is scavenged by ascorbate specific peroxidase in spinach chloroplasts. *Plant Cell Physiol*. **22**, 867-880.

Nieboer E, Richardson DHS. 1980. The replacement of the nondescript term 'heavy metal' by a biologically significant and chemically significant classification of metal ions. *Environmental Pollution* **B1,** 3–26.

Opdenakker K, Remans T, Keunen E, Vangronsveld J, Cuypers A. 2012. Exposure of *Arabidopsis thaliana* to Cd or Cu excess leads to oxidative stress mediated alterations in MAPKinase transcript levels. *Environ. Exp. Bot.* **83**, 53–61.

Peterson CA, Rauser WE. 1979. Callose Deposition and Photoassimilate Export in *Phaseolus vulgaris* Exposed to Excess Cobalt, Nickel, and Zinc. *Plant physiology*, **63**(6), 1170-1174

Pető A, Lehotai N, Lozano-Juste J, León J, Tari I, Erdei L, Kolbert Zs. 2011. Involvement of nitric oxide and auxin in signal transduction of copper-induced morphological responses in *Arabidopsis* seedlings. *Annals of botany*, **108**(3), 449-457.

Piršelová B, Mistríková V, Libantová J, Moravčíková J, Matušíková I. 2012. Study on metal-triggered callose deposition in roots of maize and soybean. *Biologia*, **67**(4), 698-705.

Potters G, Pasternak TP, Guisez Y, Jansen MA. 2009. Different stresses, similar morphogenic responses: integrating a plethora of pathways. *Plant, cell & environment*, **32**(2), 158-169.

Radi R. 2004. Nitric oxide, oxidants and protein nitration. *Proc. Natl. Acad. Sci. U.S.A.* **101**, 4003-4008

Radi R, Beckman JS, Bush KM, Freeman A. 1991. Peroxynitrite-induced membrane lipid peroxidation: The cytotoxic potential of superoxide and nitric oxide. *Archives of Biochemistry and Biophysics* **228**: 481-487

Rout GR, Das P. 2003. Effect of metal toxicity on plant growth and metabolism: I. Zinc. *Agronomie-Sciences des Productions Vegetales et de l'Environnement*, **23**(1), 3-12.

Sandalio LM, Dalurzo HC, Gómez M, Romero-Puertas MC, del Río LA. 2001. Cadmium-induced changes in the growth and oxidative metabolism of pea plants. *J. Exp. Bot.* **52** (364):2115-2126

Schützendübel A, Polle A. 2002. Plant responses to abiotic stresses: heavy metal-induced oxidative stress and protection by mycorrhization. *Journal of experimental botany*, **53**(372), 1351-1365

Signorelli S, Corpas FJ, Borsani O, Barroso JB, Monza J. 2013. Water stress induces a differential and spatially distributed nitro-oxidative stress response in roots and leaves of *Lotus japonicus*. *Plant Science*, **201**, 137-146.

Sjölund RD. 1997. The phloem sieve element: a river runs through it. *The Plant Cell*, **9**(7), 1137.

Smith JM, Dasgupta TP. 2000. Kinetics and Mechanism of the Decomposition of S-Nitrosoglutathione by Ascorbic Acid and Copper Ions in Aqueous Solution to Produce Nitric Oxide. *Nitric Oxide*, **4**(1), 57-66

Stoyanova Z, Doncheva S. 2002. The effect of zinc supply and succinate treatment on plant growth and mineral uptake in pea plant. *Braz. J. Plant Physiol*. **14**, 111–116.

Takeuchi N, Tanaka F, Katayama Y, Matsumiya K, Yamamura Y. 1976. Effects of alpha-tocopherol on thiobarbituric acid reactive substances in serum and hepatic subcellular organelles and lipid metabolism. *Exp Gerontol* **11**(5-6):179-185.

Turner RG, Marshall C. 1972. The accumulation of zinc by subcellular fractions of roots of Agrostis tenuis Sibth. in relation to zinc tolerance. *New Phytologist*, **71**(4), 671-676.

Tsukagoshi H, Busch W, Benfey PN. 2010. Transcriptional regulation of ROS controls transition from proliferation to differentiation in the root. *Cell*,**143**(4), 606-616.

Valderrama R, Corpas FJ, Carreras A, Gómez-Rodríguez MV, Chaki M, Pedrajas JR, Barroso JB. 2006. The dehydrogenase-mediated recycling of NADPH is a key antioxidant system against salt-induced oxidative stress in olive plants. *Plant, cell & environment*, **29**(7), 1449-1459.

van de Mortel JE, Villanueva LA, Schat H, Kwekkeboom J, Coughlan S, Moerland PD, Aarts, MG. 2006. Large expression differences in genes for iron and zinc homeostasis, stress response, and lignin biosynthesis distinguish roots of *Arabidopsis thaliana* and the related metal hyperaccumulator *Thlaspi caerulescens*. *Plant Physiology*, **142**(3), 1127-1147.

van der Vliet A, Eiserich JP, Shigenana MK, Cross CE. 1999. Reactive nitrogen species and tyrosine nitration in the respiratory tract: epiphenomena or a pathobiologic mechanism of disease? *Am. J. Respir. Crit. Care Med*, **160**, 1-9.

Wang C, Zhang SH, Wang PF, Hou J, Zhang WJ, Li W, Lin ZP. 2009. The effect of excess Zn on mineral nutrition and antioxidative response in rapeseed seedlings. *Chemosphere* **75**: 1468–1476

Wang Y, Loake GJ, Chu C. 2013. Cross-talk of nitric oxide and reactive oxygen species in plant programed cell death. *Frontiers in Plant Science* **4**:1-7.

White MC, Baker FD, Chaney RL, Decker AM. 1981. Metal complexation in xylem fluid. II. Theoretical equilibrium model and computational computer program. *Plant Physiology*. **67**, 301-310.

WHO. 2005. Comparative Quantification of Health Risks: Global and Regional Burden of Diseases Attributable to Selected Major Risk Factors, volt 1-3, Organizacion Mundial de la Salud

Wintz H, Fox T, Wu YY, Feng V, Chen WQ, Chang HS, Zhu T, Vulpe C. 2003. Expression profiles of *Arabidopsis thaliana* in mineral deficiencies reveal novel transporters involved in metal homeostasis. *J Biol Chem* **278**: 47644–47653

Xu J, Yin H, Li Y, Liu X. 2010. Nitric oxide is associated with long-term zinc tolerance in *Solanum nigrum*. *Plant physiology*, **154**(3), 1319-1334.

Zarcinas BA, Ishak CF, McLaughlin MJ, Cozens G. 2004. Heavy metals in soils and crops in Southeast Asia. *Environmental Geochemistry and Health*, **26**(4), 343-357.

Figures and figure legends

Fig 1 Zinc concentration (μg g^{-1} DW) in roots (A) and shoots (B) of control and zinc-exposed *B. juncea* and *B. napus* plants. Significant differences with respect to control plants (5 □M $ZnSO_4$) and according to Student's t-test (n = 10, ***P ≤ 0.001) are indicated.

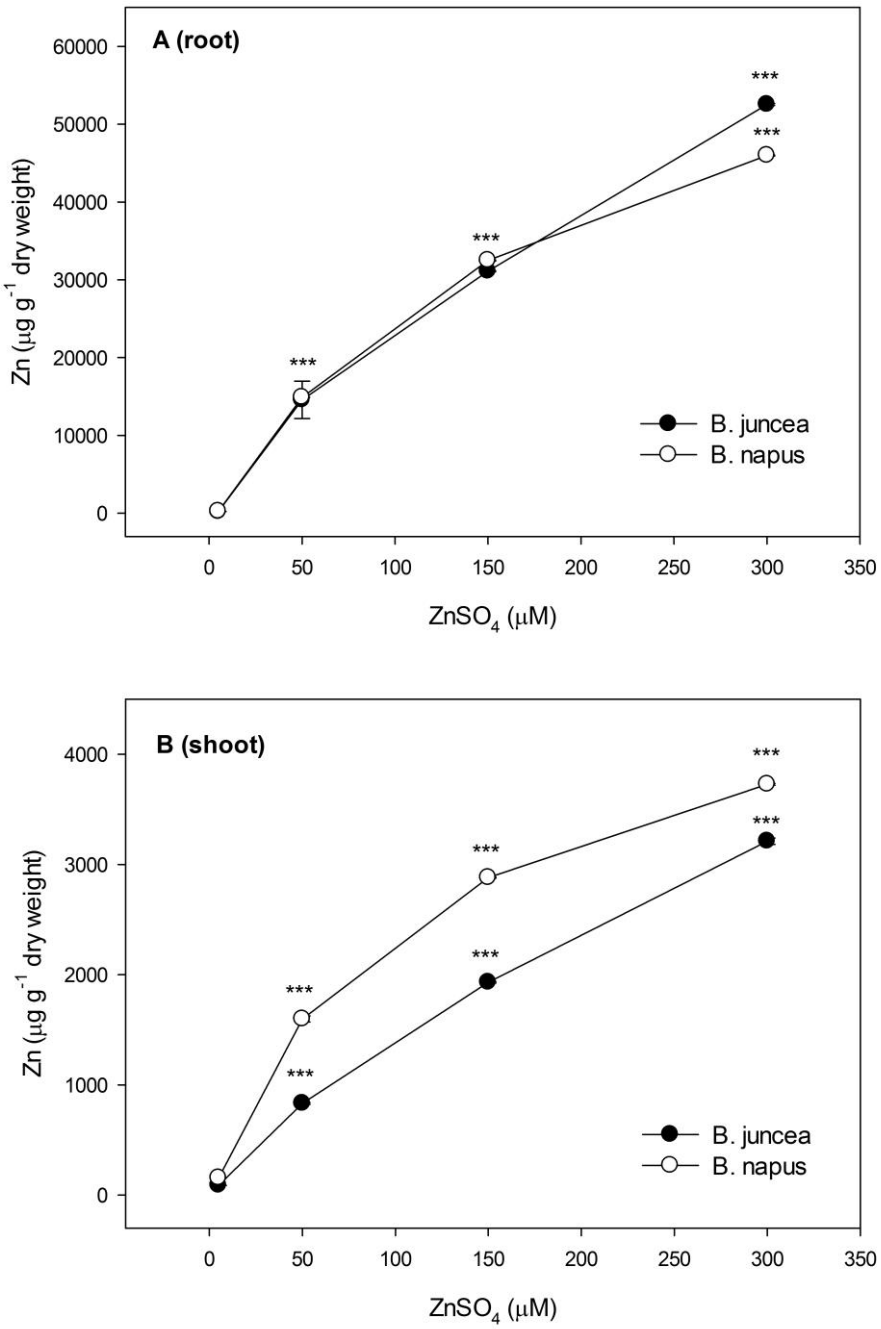

Fig 2 (A) Tissue specificity of zinc localization in control and zinc-treated *Brassica juncea* and *Brassica napus* root tips. Zinc localization was visualized with the help of Zinquin fluorophore as described in *Materials and methods.* Bar=200µm (B) Pixel intensities of Zinquin fluorescence measured in the PR meristem of control and Zn-treated *Brassica* species. Different letters indicate significant differences according to Duncan-test (n = 10, P≤0.05).

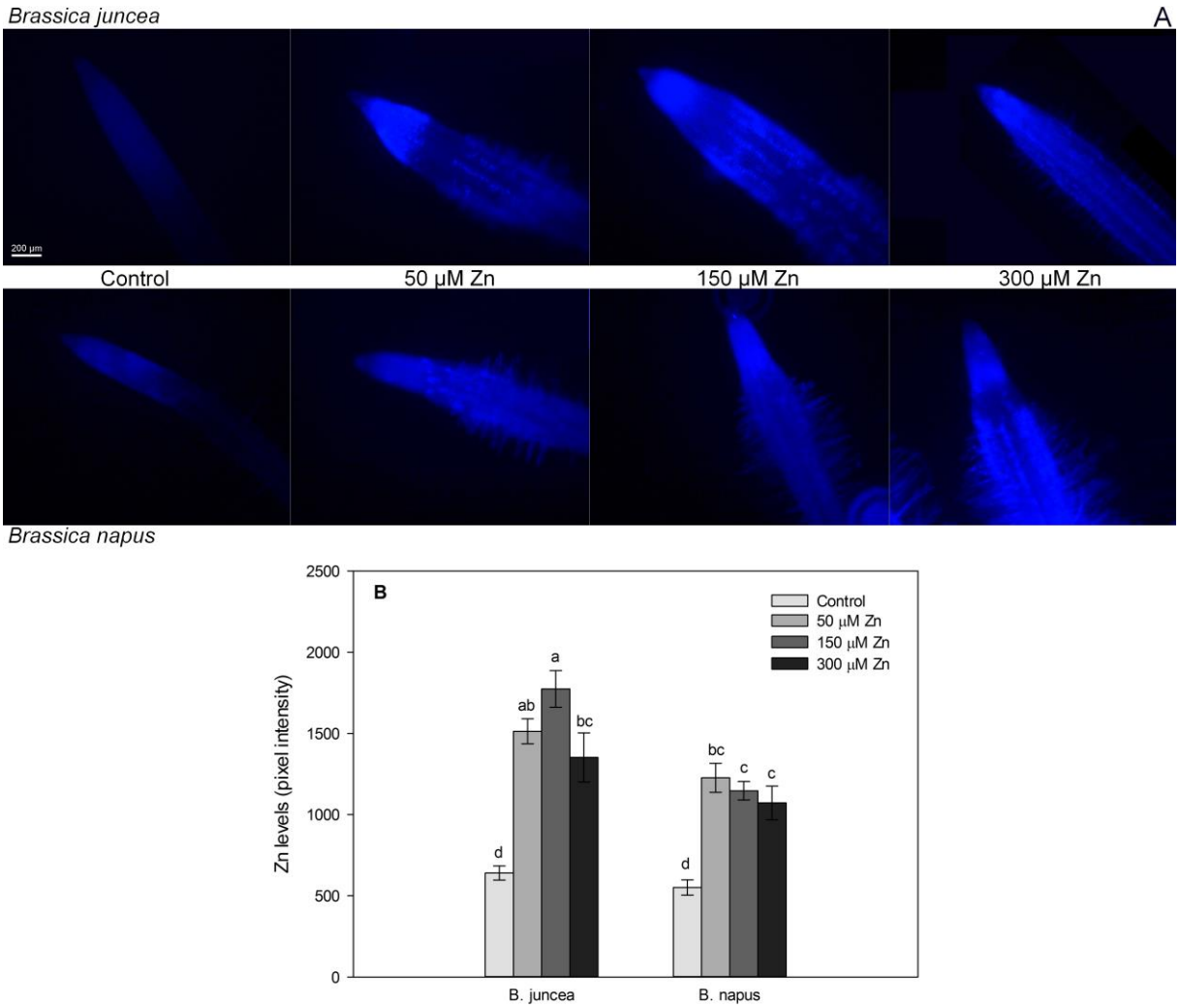

Fig 3 Confocal microscopic images of the root tip of 300 µM Zn-treated *B. juncea*. The root samples were co-stained with Zinpyr-1 and PI. (A) Lower magnification merged image of the whole root tip (A) and optically zoomed image showing root epidermal cells (B). Green

(ZinPyr) fluorescence corresponds to zinc (C) and red (PI) fluorescence shows cell walls and nuclei (D). Bars=100 µm.

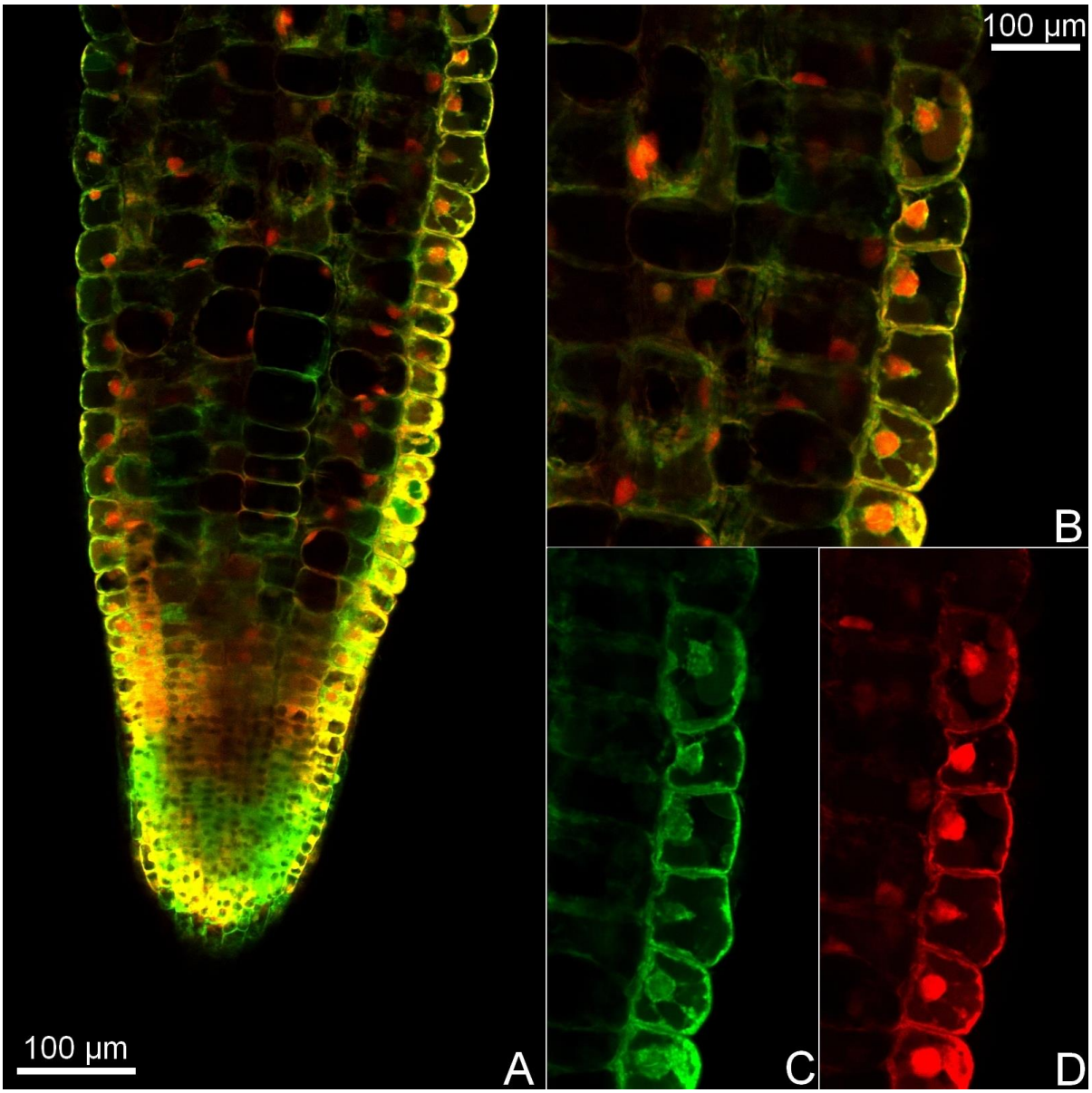

Fig 4 The effect of excess Zn on the growth of *B. juncea* and *B. napus* plants. (A) Representative photographs of 16-days-old untreated and zinc-exposed *B. juncea* and *B. napus* plants. Bar=1 cm. Primary root length in control % (B), number (C) and length (D) of lateral roots and root fresh weight in control% (E) of *Brassica* plants treated with 0, 50, 150 or 300 µM Zn. The lack of significance (n.s.) or significant differences according to Student's t-test (n = 20, **P≤0.01, ***P ≤ 0.001) are indicated.

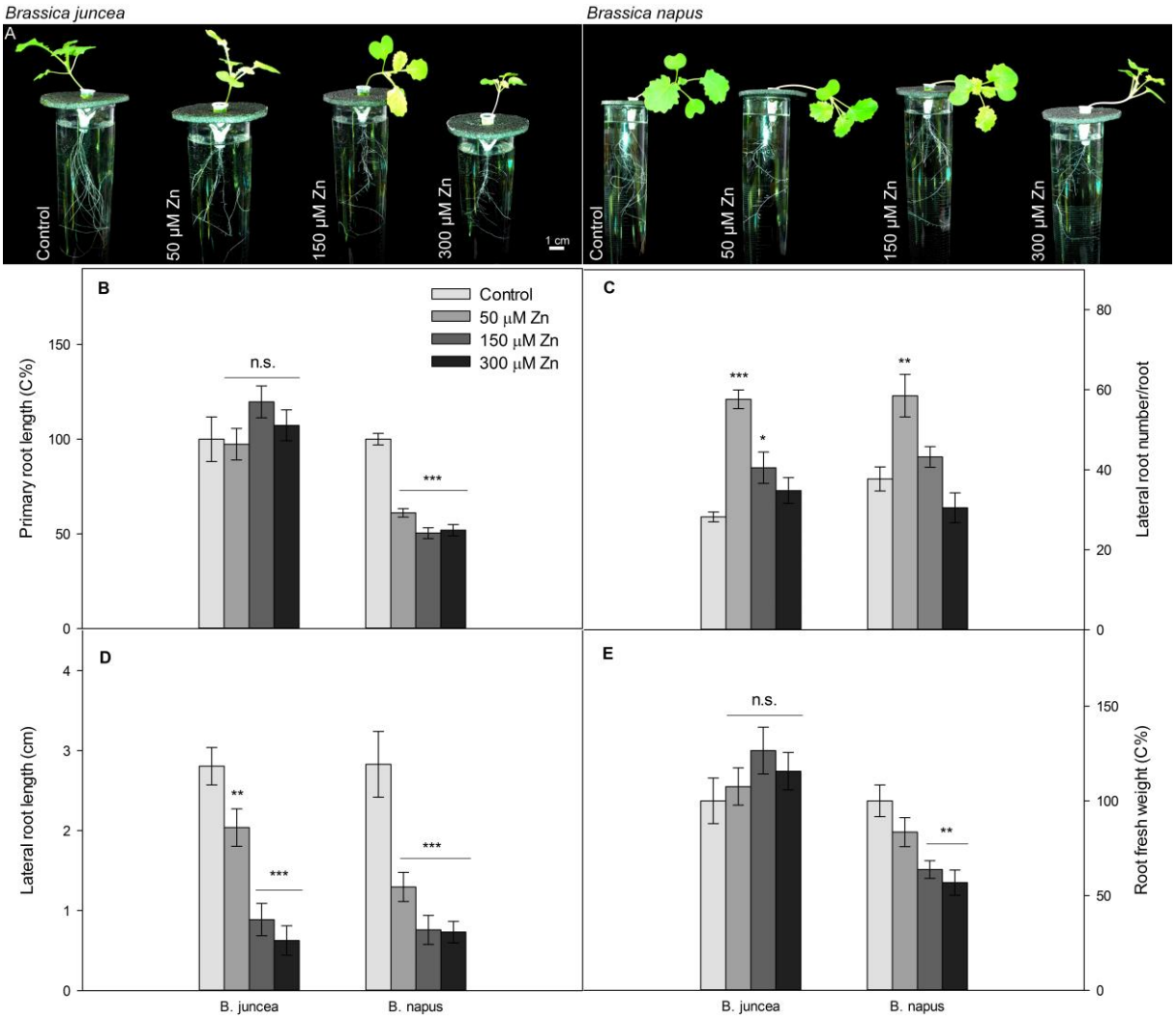

Fig 5 Intensity of anilin blue-dependent fluorescence (in control %) reflecting callose levels in the root tips of control and zinc-treated *Brassica* plants. Significant differences according to Student's t-test (n = 10, *P≤0.05, **P≤0.01, ***P ≤ 0.001) are indicated.

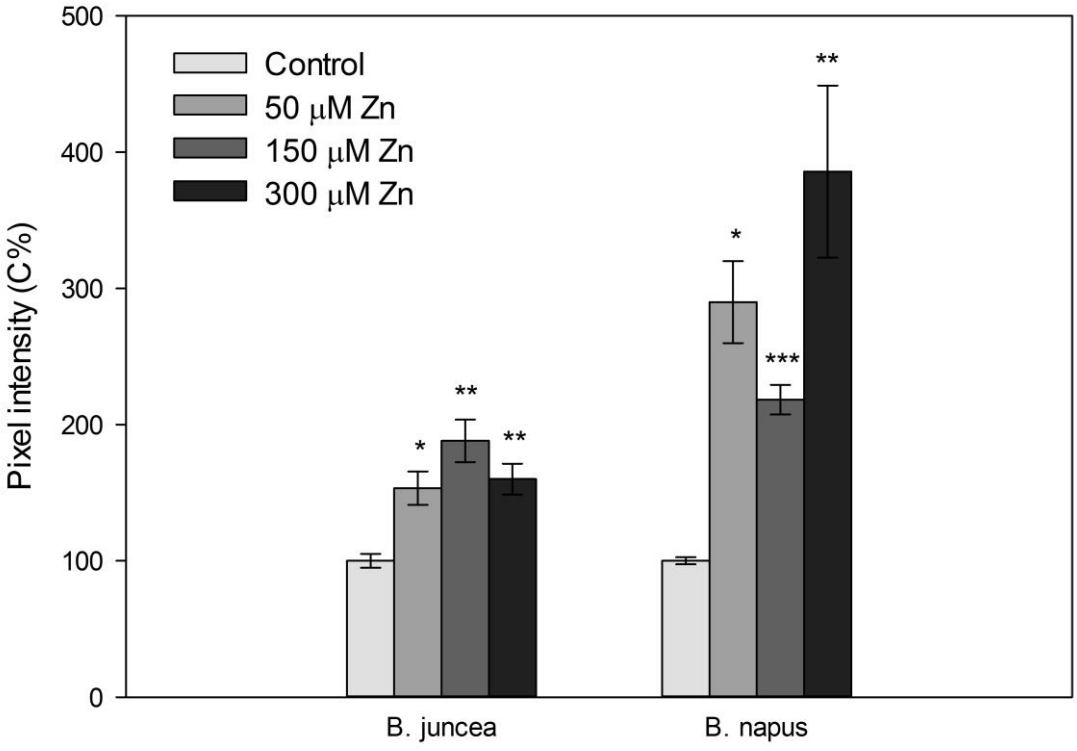

Fig 6 Viability (fluorescein pixel intensities in control %) of the root meristem cells of control and zinc-exposed *Brassica* plants. The lack of significance (n.s.) or significant differences according to Student's t-test (n = 10, *P≤0.05, **P≤0.01, ***P ≤ 0.001) are indicated.

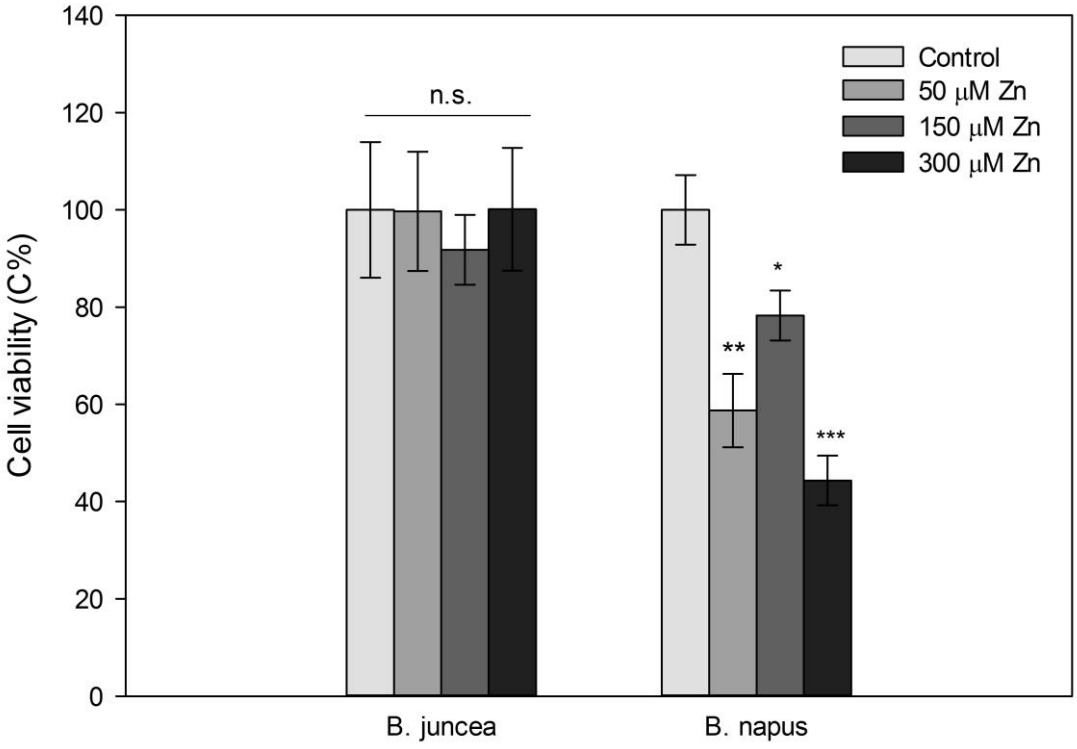

Fig 7 Effect of Zn excess on the metabolism of ROS and RNS. The levels of superoxide radicals (pixel intensity of DHE fluorescence, A), total SOD activity (B), H_2O_2 (pixel intensity of resorufin fluorescence, C), APX activity (D), NO (pixel intensity of DAF-FM fluorescence, E) and $ONOO^-$ (pixel intensity of APF fluorescence, F) in control and zinc-treated *Brassica* roots (in meristematic zone) are shown. (G) Representative microscopic images of *Brassica* root tips stained with different fluorophores (from left: DHE for superoxide in *B. napus*, Ampliflu^{TM} for H_2O_2 in *B. napus*, DAF-FM for NO in *B. napus*, APF for ONOO- in *B. napus*). The fluorescent staining procedures were carried out in the root tips, while enzymatic activities were measured in the whole root system as described in *Materials and methods*. Different letters indicate significant differences according to Duncan-test (n = 10, $P \leq 0.05$).

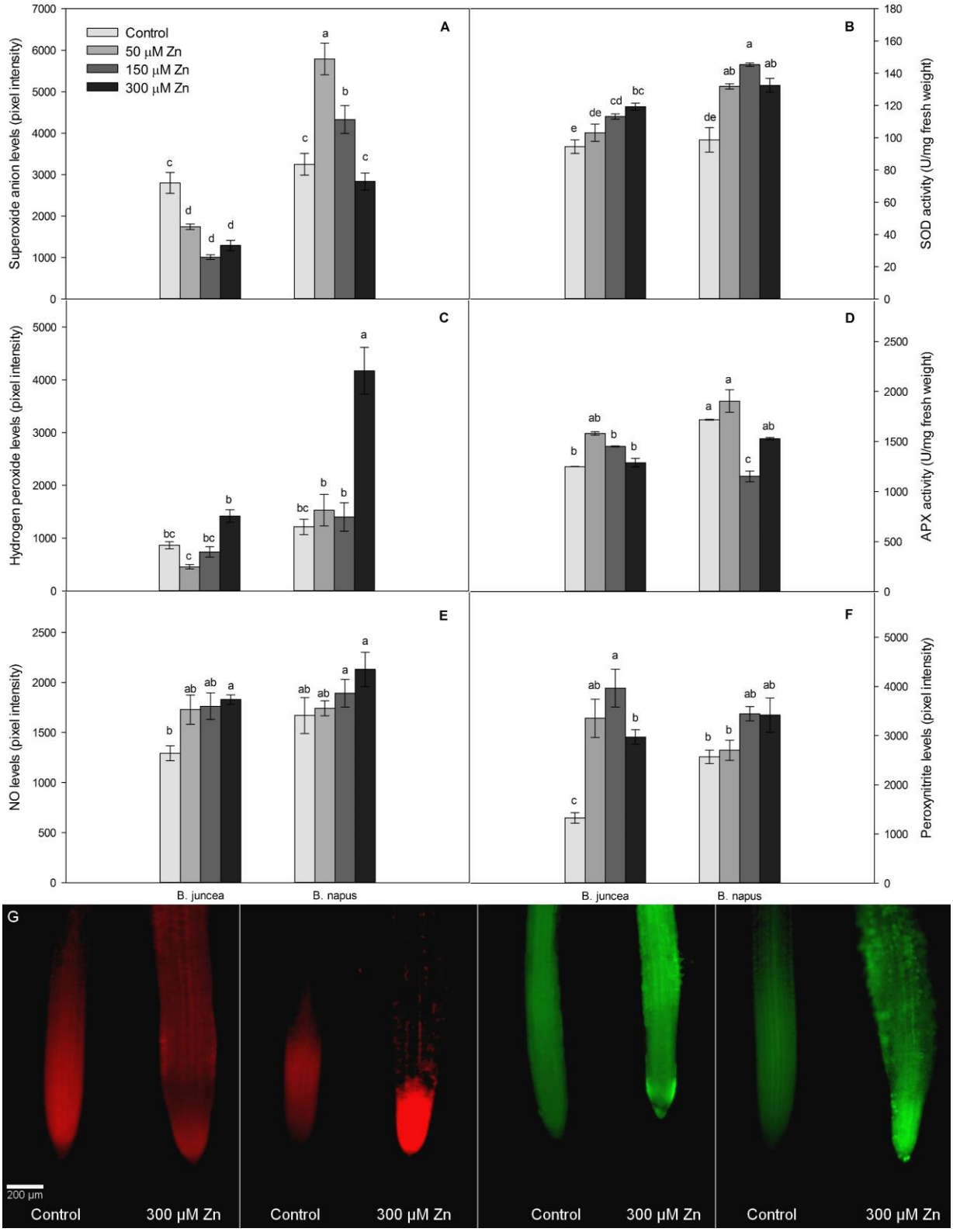

Fig 8 Analysis of SOD isoforms. SOD isoforms were separated by native-PAGE and stained by a photochemical method using 30 μg of protein per lane.

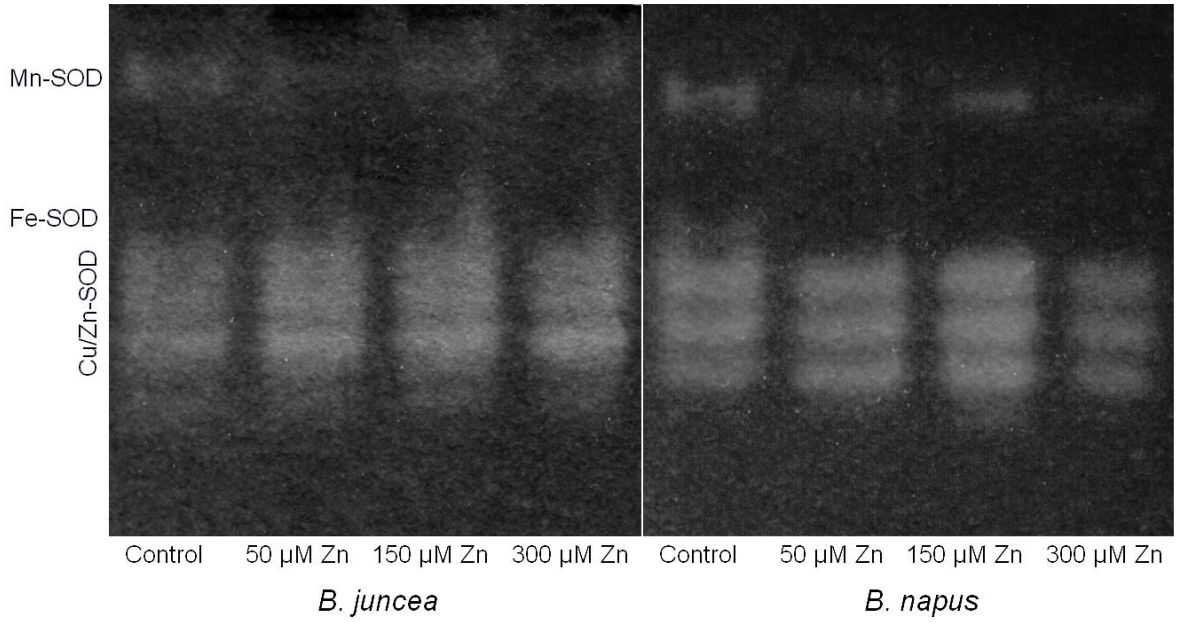

Fig 9 Representative immunoblots showing protein tyrosine nitration in roots of *B. juncea* and *B. napus* plants under control circumstances and subjected to 300 µM Zn. Root samples were separated by SDS-PAGE and analysed on Western blotting with anti-nitrotyrosine antibody (1:2000). Commercial nitrated BSA (NO_2-BSA) was used as a positive control.

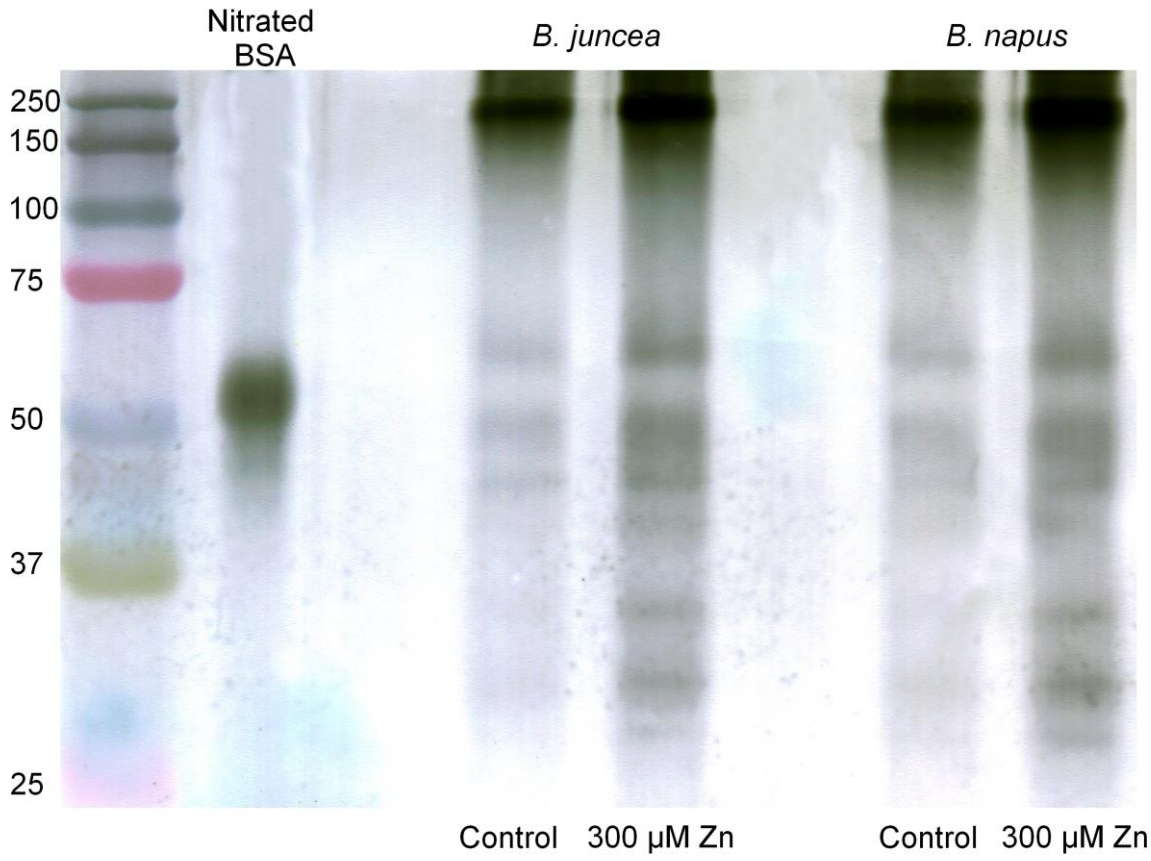

Fig 10 Microscopic images of *Brassica* root tips stained with the Schiff's reagent. The pink colorization indicates lipid peroxidation. Bar=200 μm.

Table 1 Copper (Cu), manganese (Mn) and iron (Fe) concentrations ($\mu g \cdot g^{-1}$ DW) in roots of control and zinc-treated *Brassica* plants. Significant differences according to Student's t-test (n = 10, ***P ≤ 0.001) are indicated.

			Brassica juncea			
	Control	50 µM Zn		150 µM Zn		300 µM Zn	
Cu	24.50 ± 0.38	173.00 ± 0.52		198.90 ± 0.49		174.80 ± 0.73	
Mn	250.00 ± 1.16	24.97 ± 0.05	***	25.53 ± 0.07	***	26.02 ± 0.13	***
Fe	519.10 ± 4.75	864.50 ± 3.65		869.90 ± 2.71		927.90 ± 2.22	
			Brassica napus			
	Control	50 µM Zn		150 µM Zn		300 µM Zn	
Cu	27.68 ± 0.08	150.60 ± 0.50		178.60 ± 0.85		163.70 ± 0.68	
Mn	145.10 ± 0.53	26.40 ± 0.09	***	22.02 ± 0.10		26.44 ± 0.17	***
Fe	1051.0 ± 4.5	1496.0 ± 6.7		1540.0 ± 11.3		1239.0 ± 7.8	